

## RESEARCH ARTICLE OPEN ACCESS

# Performance of Seismically Isolated and Non-Isolated Steel-Framed Buildings: Sensitivity to Amount and Form of Inherent Damping

Shoma Kitayama<sup>1</sup> | Michael C. Constantinou<sup>2</sup>

<sup>1</sup>Department of Civil and Environmental Engineering, Brunel University of London, Uxbridge, UK | <sup>2</sup>Department of Civil, Structural and Environmental Engineering, University at Buffalo, State University of New York, Buffalo, New York, USA

**Correspondence:** Shoma Kitayama ([shoma.kitayama@brunel.ac.uk](mailto:shoma.kitayama@brunel.ac.uk))

**Received:** 1 October 2024 | **Revised:** 24 February 2025 | **Accepted:** 26 March 2025

**Funding:** The authors received no specific funding for this work.

**Keywords:** collapse | inherent damping | seismic isolation | seismic performance | sensitivity | steel structures

## ABSTRACT

The amount of inherent damping assumed in nonlinear response history analysis of steel buildings is typically set at 2% or less for the fundamental mode of vibration. However, many studies have shown that actual damping levels vary depending on the building characteristics and soil conditions, and methodologies used in measurements of damping in the field. Reported inherent damping values range from 1% to more than 5% for the fundamental mode of vibration. This study investigates the effects on the computed seismic performance of the assumed level and form of inherent damping in nonlinear response history analysis, focusing on seismically isolated and non-isolated buildings with special moment-resisting and concentrically braced frames. The seismic isolation systems considered are sliding friction pendulum type. The findings demonstrate that the assumed value of inherent damping has an impact on the computed floor accelerations, affecting acceleration-sensitive non-structural components, particularly with periods less than 1 s. Collapse probabilities of isolated buildings are minimally affected by the assumption of inherent damping, leading to simplifying modeling for collapse-focused analyses. Comparative studies involving conventional non-isolated buildings reveal significant sensitivity to inherent damping values across various metrics, including floor accelerations, peak story drift ratios, residual drift ratios, and collapse probabilities. It is shown that non-isolated building models exhibit reduced sensitivity of collapse probabilities and floor spectral accelerations when inherent damping is specified using different methods—specifically, capped viscous damping as compared to modal damping. This highlights that while the performance of seismically isolated buildings shows relatively small sensitivity to the model of inherent damping, non-isolated buildings exhibit notable differences.

## 1 | Introduction

The amount of inherent damping used for nonlinear response history analysis of steel buildings is usually assumed to be 2% for all modes of vibration. However, recent studies indicated that different damping values are more representative of

the actual behavior of buildings depending primarily on their height, construction methods, materials, and soil conditions. Additionally, these studies reported that the method of measurement of damping affected the results, indicating an even greater uncertainty in values. Some of these works are reviewed below.

This is an open access article under the terms of the [Creative Commons Attribution](https://creativecommons.org/licenses/by/4.0/) License, which permits use, distribution and reproduction in any medium, provided the original work is properly cited.

© 2025 The Author(s). *Earthquake Engineering & Structural Dynamics* published by John Wiley & Sons Ltd.

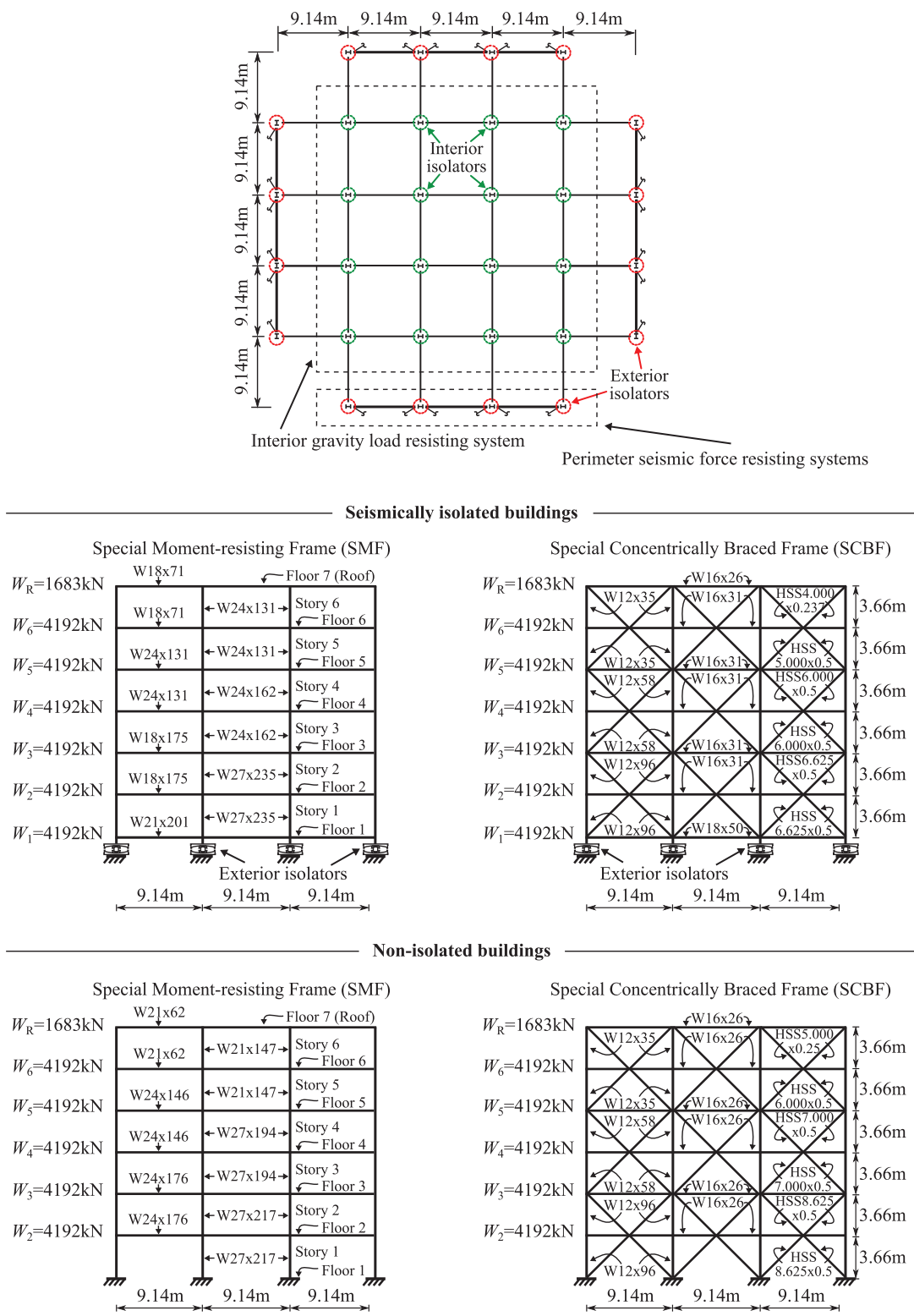


**FIGURE 1** | Plan and elevation views of analyzed buildings.

An early study by Satake et al. [1] used data from forced vibration testing, and wind and earthquake-induced vibration records in Japanese buildings, to demonstrate that inherent damping in steel-framed buildings is lower than in reinforced concrete buildings. The study found that inherent damping ratio values in the fundamental mode vary from 0.5% to 8% of critical, depending on the materials used and the height of the building. A later

study [2] reported that the amount of inherent damping varies depending on the cause of the building vibrations, whether from forced vibration, wind, or earthquake-induced vibrations. This suggests that the appropriate inherent damping for seismic nonlinear response history analysis should be determined based on data obtained from earthquake-induced vibrations. Consequently, recent studies have used data on building response



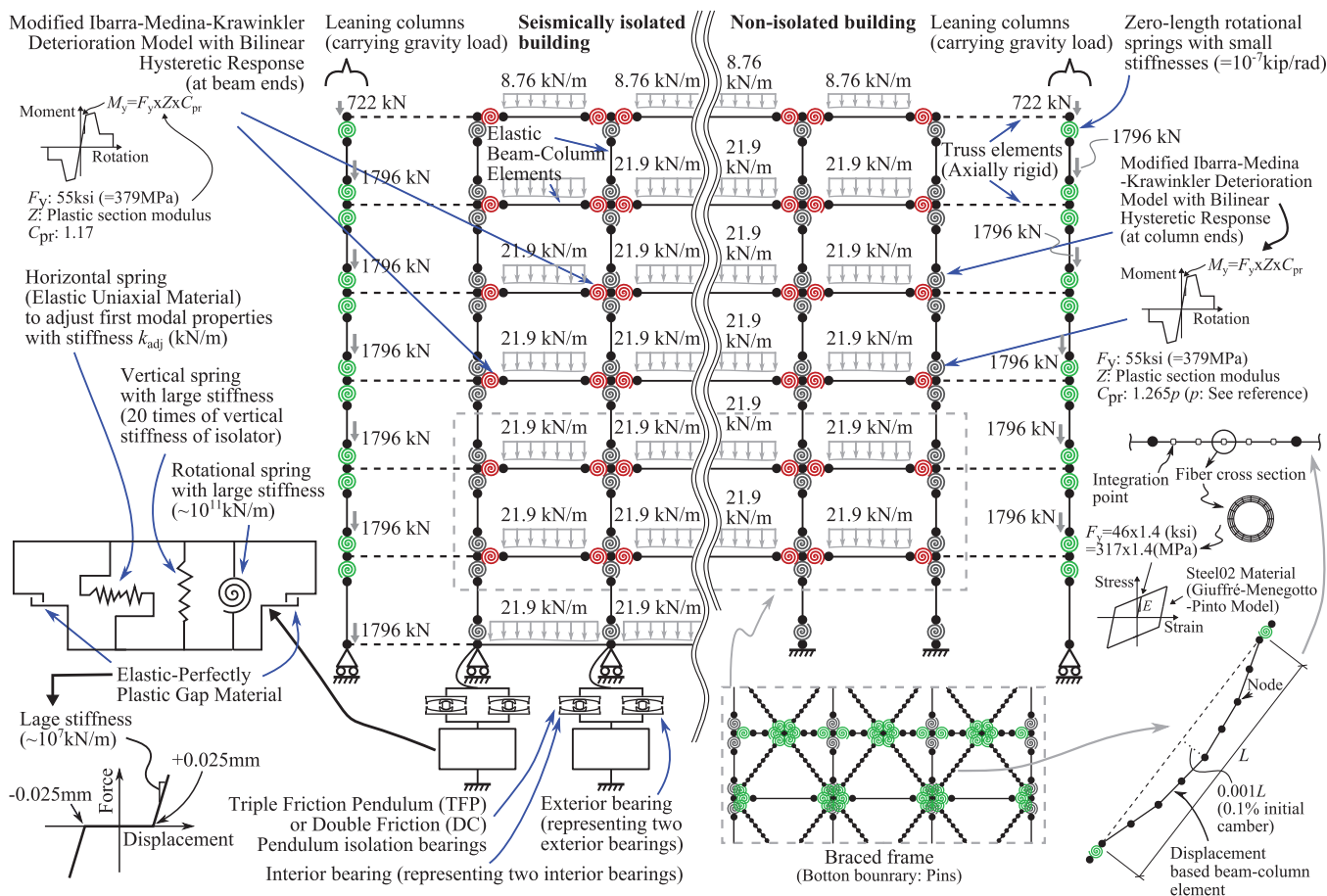


**FIGURE 3** | Model of six-story seismically isolated and non-isolated buildings.

In summary, a range of values for inherent damping is recommended for use in nonlinear response history analysis of buildings. This study aims to contribute toward understanding of how seismic performance is affected by the assumed amount of inherent damping in nonlinear response history analysis. The study follows the paradigm of a recent study by the authors (Kitayama and Constantinou [13]), using the same building models (but for some improvements based on the most contemporary structural element models) and seismic hazard characterization and varies the amount of damping assumed in the analysis for two different cases of damping model. The buildings are seismically isolated 6-story buildings with special moment resisting frames (SMF) and special concentrically braced frames (SCBF) and comparable non-isolated buildings, designed for the same location as the seismically isolated buildings. The seismic isolation systems considered are sliding friction pendulum of the Triple and Double types that satisfy the minimum requirements of standards ASCE/SEI 7-16 and 7-22 [14, 15]. The systems, in some cases, were provided with moat walls. These isolation systems were selected because a considerable body of knowledge exists on the seismic performance, including collapse performance, of buildings with these isolators [13, 16–18], on which this study could build on. The study could not be extended to other isolation systems as a complete redesign of the structural systems would have been needed, and validated models of collapse behavior of the isolators would have been required to be described.

The findings of this study offer insight into the appropriate specification of inherent damping for seismic performance evaluation across various building types and for different metrics of seismic performance assessment. The results are valid for the isolation systems studied and do not necessarily apply to all isolation systems.

## 2 | Description of Analyzed Buildings

Plan and elevation views of the analyzed buildings are shown in Figure 1. The original design of this building was presented in SEAONC Volume 5 Seismic Design Manual [19] and McVitty and Constantinou [20] and later modified by Kitayama and Constantinou [16–18]. The total seismic weight of the building when seismically isolated is 53,670 kN. When non-isolated the weight is 45,285 kN. The building is assumed to be located at a site in California with Risk-Targeted Maximum Considered Earthquake ( $MCE_R$ ; ASCE, 2017, 2021) spectral acceleration values of  $S_{MS} = 1.5$  g and  $S_{M1} = 0.9$  g. The seismic force-resisting frames for the isolated buildings were designed for  $R_1 = 2$ , ensuring minimal compliance with the design requirements in ASCE/SEI 7-16 [14]. Comparable non-isolated buildings were designed for  $R = 6$  (SCBF) or 8 (SMF) based on Section 12 of ASCE/SEI 7-16 [14] using the Design Earthquake (DE [14]) with parameters  $S_{DS} = 1.0$  g and  $S_{D1} = 0.6$  g. The designs also satisfy the criteria of ASCE/SEI 7-22 [15] provided that the spectral acceleration values are the same (based on ASCE 7-16, these spectral values

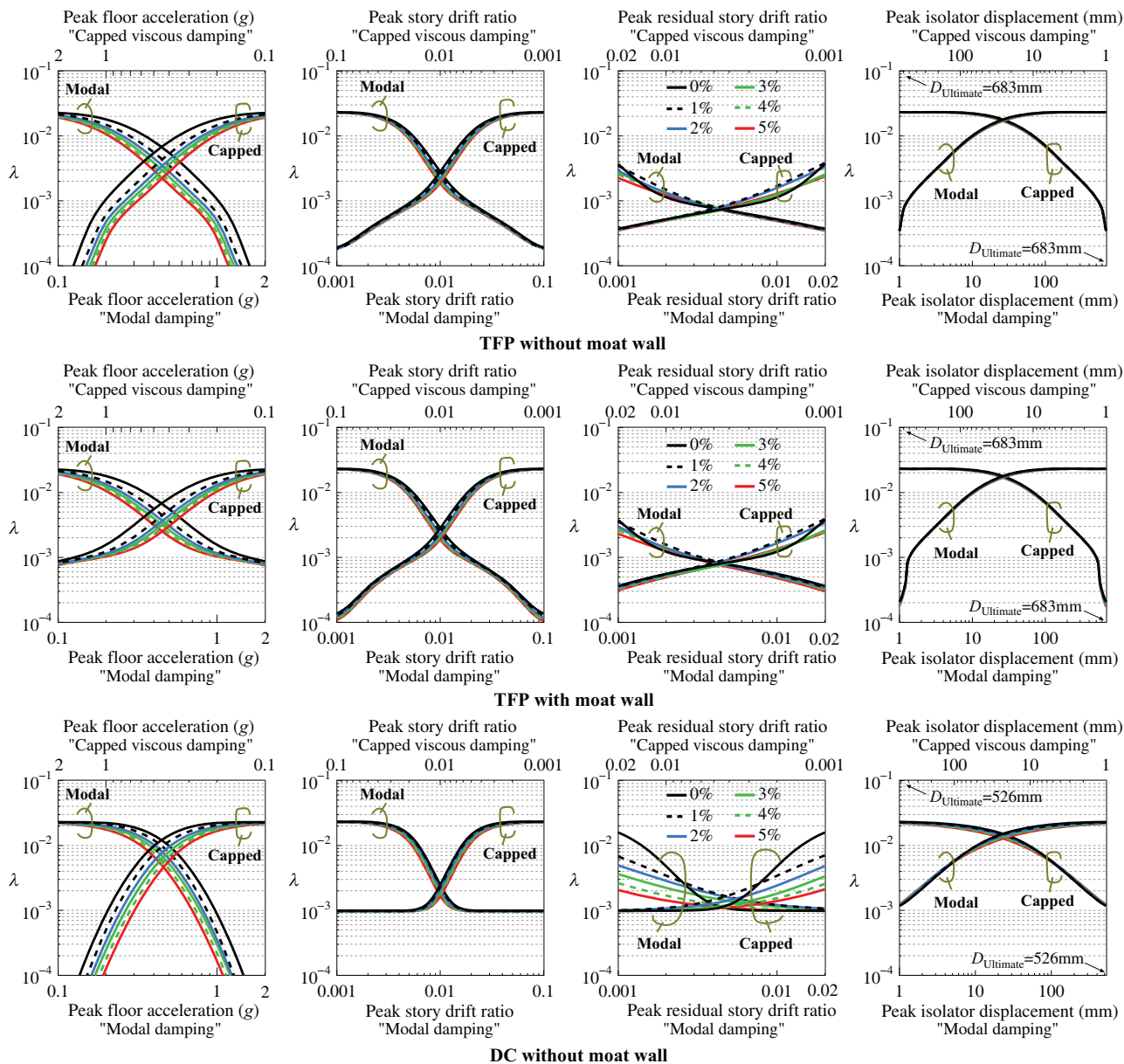


**FIGURE 4** | Mean annual frequencies of exceedance for various engineering demand parameters (EDP) of seismically isolated buildings with special moment resisting frames (SMF).

are for soil class D at a location with latitude  $37.783^\circ$ , longitude  $-122.392^\circ$ ). Note that beam sections shown in Figure 1 extend over three bays. The designed seismic isolation systems are shown in Figure 2. They meet the minimum requirements of ASCE/SEI 7-16 and 7-22, with the double concave (DC) system just meeting the minimum requirements (displacement capacity at collapse just over the average demand  $D_M$ ) and without a moat wall. The triple friction pendulum (TFP) system meets the minimum requirements but also has the additional capacity to deform by  $0.3D_M$  in its stiffening regime. Additional analyses were performed with the TFP system when a moat wall was used to be active for displacements larger than  $D_M$ , as shown in the loops of Figure 2, to prevent the collapse of the isolators. The DC system with a moat wall placed so that it is active for displacements larger than  $D_M$ , has a collapse behavior identical to the TFP system with the same moat wall (note that  $D_M$  is the same for both systems)-however, the DC system needs then to have

larger displacement capacity for the moat wall to be effective. The DC and the TFP systems (with behavior as shown in Figure 2) only differ in behavior when displacements are very small or when unloading occurs for displacements less than  $D_M$  (when the TFP has motion at its inner sliding surfaces). This difference in behavior has effects on the acceleration response and on residual displacements, which are smaller for the TFP system. Additional details of the design of the seismically isolated and non-isolated buildings may be found in Kitayama and Constantinou [16, 17]. Note that parameter  $D_M$  ( $= 518$  mm) was determined based on response history analysis and simplified analysis following procedures in ASCE/SEI 7-16. The simplified analysis procedures are identical in ASCE/SEI 7-16 and 7-22, but the response history analysis procedures differ in the number of ground motions (11 instead of 7) and in terms of how ground motions are scaled. We presume the differences to be insignificant in the computation of  $D_M$  by the procedures of the two standards.

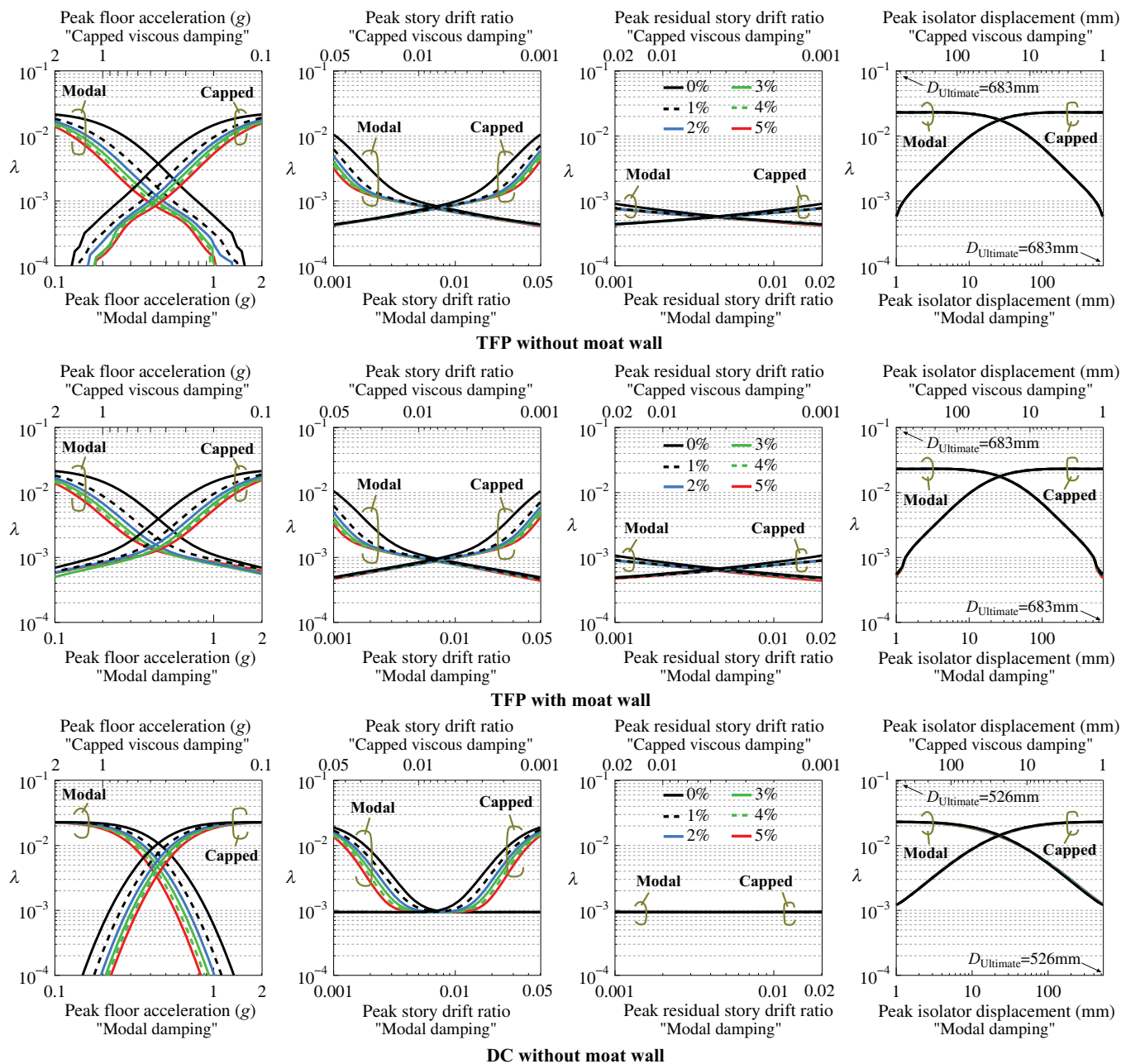


**FIGURE 5** | Mean annual frequencies of exceedance for various engineering demand parameters (EDP) of seismically isolated buildings with special concentrically braced frames (SCBF).

### 3 | Model for Analysis

The analysis was performed in the program Open System for Earthquake Engineering Simulation (OpenSees) [21] using two-dimensional representations of the structures. Figure 3 presents the models for the seismically isolated and the non-isolated buildings. The dead load was applied after the installation of the braces and before the initiation of response history analysis. The models used in this study are the same as those that were used in the previous studies of the authors [13] but utilizing a new column hinge model that can better simulate the cyclic deterioration behavior of columns after reaching their post-peak strength per Lignos et al. [22], who developed and implemented the model in OpenSees. The models used in representing the building utilized

concentrated plasticity elements (nonlinear spring hinges) for the beams and columns and distributed plasticity elements (fiber sections) for the braces. The elastic stiffness of beam-column elements between the concentrated plasticity springs was selected based on Ibarra and Krawinkler [23] so that the equivalent stiffness of the “rotational spring—elastic beam-column element—rotational spring” assembly was equivalent to the stiffness of the actual frame members. Details of models for the analysis of buildings may be found in Kitayama and Constantinou [13]. The inherent damping was specified using two methods of the many evaluated by Kitayama and Constantinou [13]:

1. The “modal damping” model with the same specified value of the damping ratio in all modes, except for the isolated

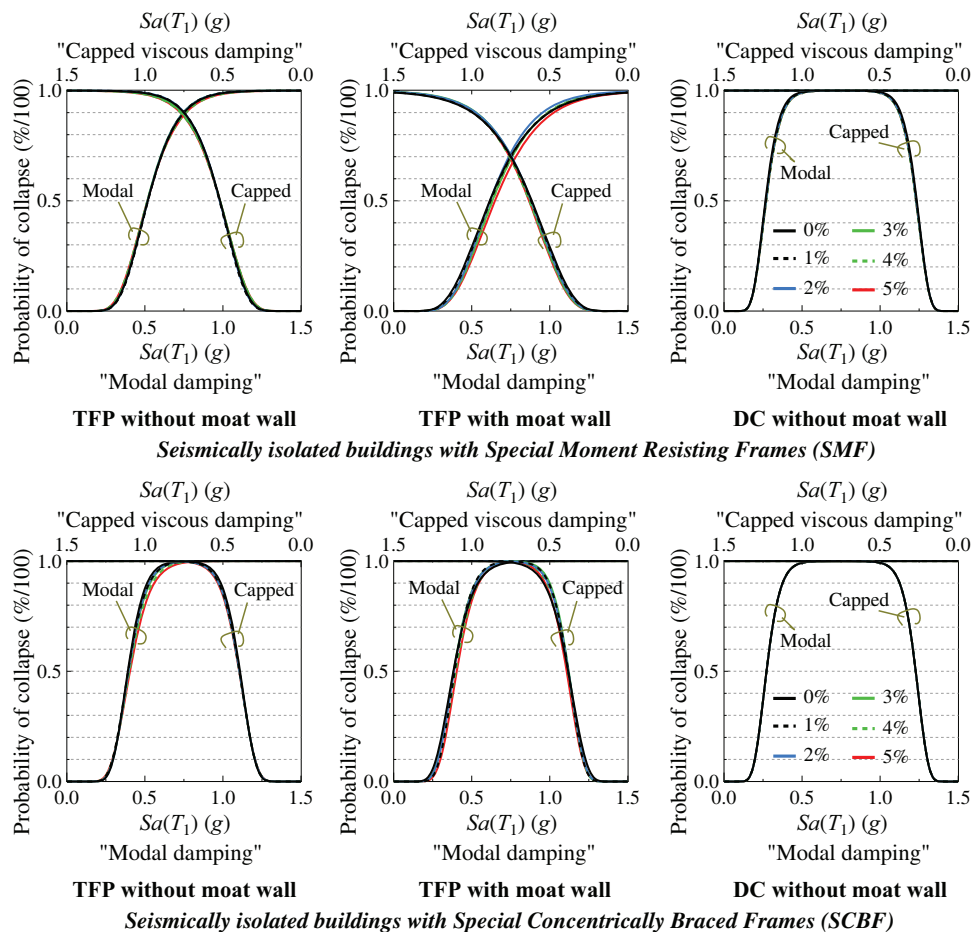


**FIGURE 6** | Collapse fragility curves of seismically isolated buildings for different amounts of inherent damping.

**TABLE 1** | Collapse probabilities (in%) of seismically isolated buildings in  $MCE_R$  ( $P_{Collapse, MCE}$ ).

System Damping ratio	SMF (modal damping/capped damping)			SCBF (modal damping/capped damping)		
	TFP without moat wall	TFP with moat wall	DC without moat wall	TFP without moat wall	TFP with moat wall	DC without moat wall
0%	3.7/3.7	2.8/2.8	42.4/42.4	10.5/10.5	13.6/13.6	39.8/39.8
1%	3.5/3.3	2.6/2.6	41.5/41.5	10.9/10.4	10.8/11.9	39.8/39.8
2%	3.6/3/5	2.1/2.3	41.5/41.5	10.4/10.4	11.9/12.4	39.8/39.8
3%	3.7/4.1	2.1/2.1	40.9/40.9	10.4/10.4	12.2/12.2	39.8/39.8
4%	4.2/4.2	1.9/2.1	40.9/40.9	10.3/10.4	10.7/12.1	39.8/39.8
5%	4.2/4.2	1.9/1.9	40.9/40.9	10.3/10.4	9.6/11.1	39.8/39.8

Abbreviations: DC, double concave; SCBF, special concentrically braced frames; SMF, special moment resisting frames; TFP, triple friction pendulum.

structures where the damping ratio was specified as zero for the “purely isolated” modes (see guidelines in [24] and details of the implementation in OpenSees in [13]). In the application of this procedure in this study, a single value of damping ratio was used for all modes of vibration.

- The “capped viscous damping” model, in which virtual linear viscous dampers are used to model inherent damping with the limits to the damping forces as described in Qian et al. [25] and originally proposed by Hall [26, 27]. The virtual dampers

were assigned limits on the positive and negative damping forces (“caps”). These forces were capped at  $2\zeta$  times the yield strength of each story (obtained in push-over analysis), where  $\zeta$  is the assumed damping ratio. This value of the damping ratio was used to compute the virtual linear viscous damper constants using the modal properties (period and mode shape) of a mode of vibration, say the  $m^{\text{th}}$  mode. For the isolated buildings, the procedure was applied by using the modal properties of the second mode of vibration, whereas for the non-isolated buildings, the modal properties of the

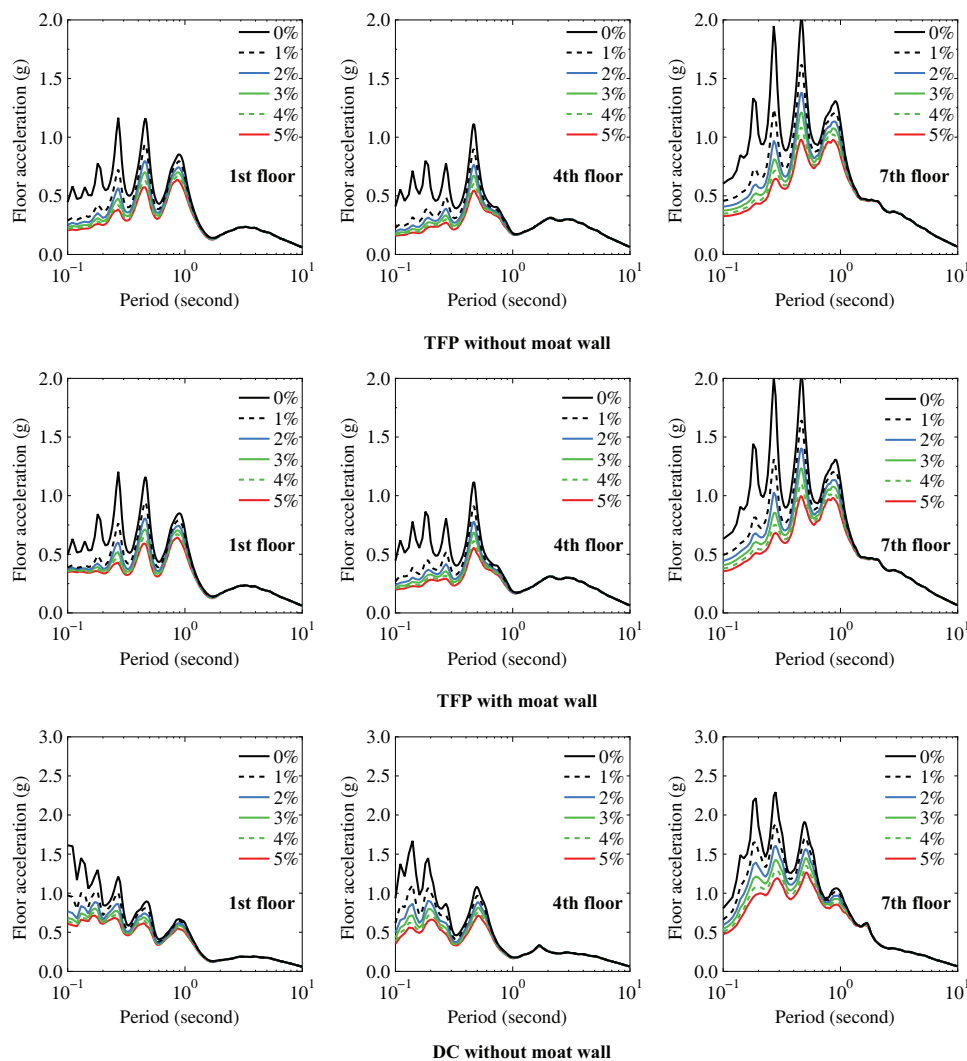


**FIGURE 7** | Mean floor acceleration spectra of seismically isolated buildings with special moment resisting frames (SMF) in 475-year return period ground motions for varying values of inherent damping modeled using “modal damping”.

first mode were used (see Kitayama and Constantinou [13] for details of the procedure). This procedure does not result in the same value of the damping ratio for each mode of vibration. It only ensures that the damping ratio is equal to the value  $\zeta$  at the  $m^{\text{th}}$  mode ( $m = 1$  for non-isolated, and  $m = 2$  for isolated structures in this study).

Note that the inherent damping models were selected based on a previous study by the authors [13] to satisfy the following conditions: (i) the “spurious damping” problem in the isolation system is eliminated or minimized, (ii) the action of hysteretic or frictional damping in either the structural elements or the seismic isolation system not duplicated, and (iii) the computational cost of inelastic time-history analysis is not substantially increased. The two inherent damping models considered in this study (capped viscous damping as compared to modal damping) are two of the recommended inherent damping models for non-isolated buildings in a recent study by Qian et al. [25].

The tangent stiffness proportional damping (i.e., using a stiffness matrix that is updated in every time step) was not considered in the current study as it was observed in past studies [13]

that (i) there was a substantial increase in the computational time for inelastic time-history analysis, and (ii) there were frequent numerical convergence problems. Also, the use of the tangent stiffness matrix to construct a damping matrix lacks a physical basis [25, 28] and, thus, was avoided in this study. A comprehensive review of available inherent damping models for seismically isolated and non-isolated buildings can be found in a previous study by the authors [13].

#### 4 | Selection and Scaling of Ground Motions for Nonlinear Response History Analysis

The ground motion records used for nonlinear response history analysis are identical to those used in previous studies by authors [13, 16, 18]. Background information is available in NIST [29] and Lin et al. [30]. A total of 400 ground motions were selected and scaled to represent ten different seismic intensities (40 records for each intensity), corresponding to earthquake return periods of 43, 144, 289, 475, 949, 1485, 2475, 3899, 7462, and 10,000 years. These intensities were measured for a period of 3.660 s, corresponding to the effective period  $T_M$  at the maximum isolator

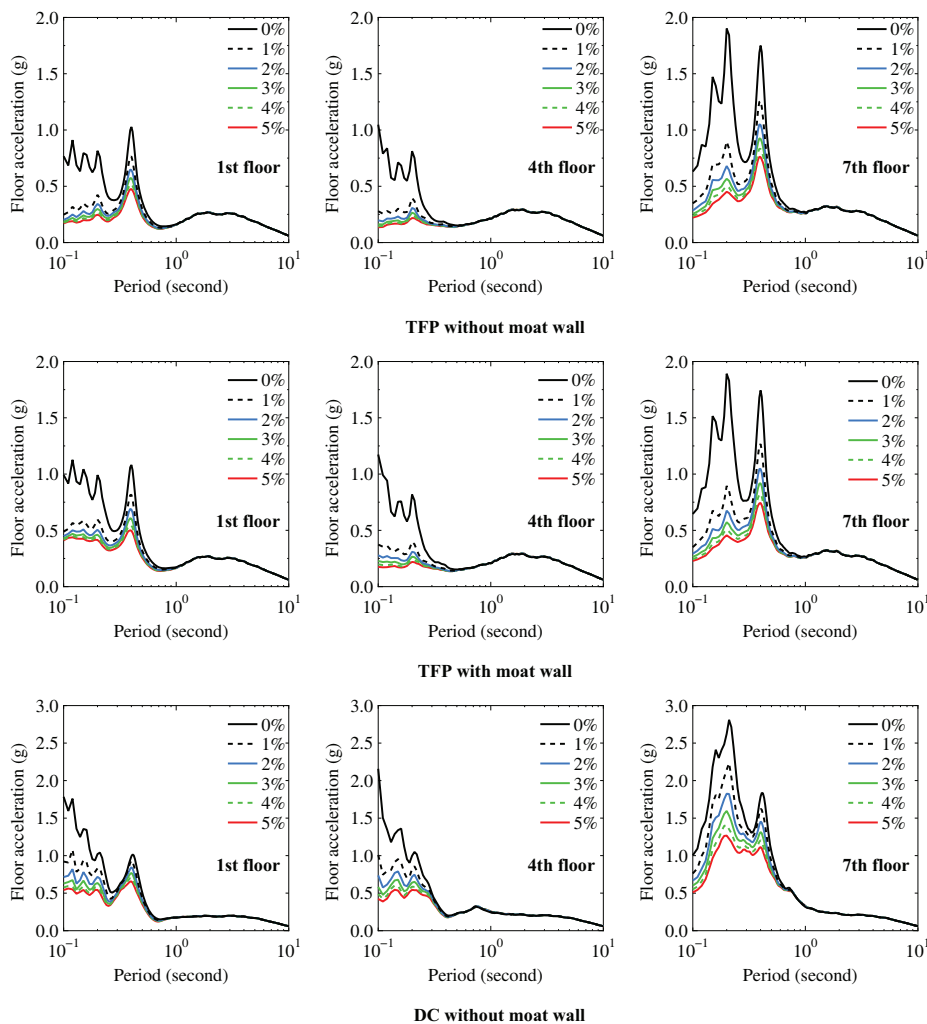


**FIGURE 8** | Mean floor acceleration spectra of seismically isolated buildings with special concentrically braced frames (SCBF) in 475-year return period ground motions modeled using “modal damping”.

displacement  $D_M$  (as per Section 17.5.3.2 in ASCE/SEI 7-16 and 7-22) for the seismically isolated buildings, and for periods of 1.186 and 0.524 s, corresponding to the first-mode periods of the non-isolated buildings with SMF and SCBF, respectively. The multiple stripe analysis technique (Jalayer [31]) was employed as it allowed for the use of different sets of hazard-consistent ground motions at each intensity level (i.e., return period). The results are presented as relationships between specific values of engineering demand parameters (EDP) and the annual frequency of exceeding these EDP values. Details on the ground motion selection and scaling for the studied structures can be found in Kitayama and Constantinou [16, 18].

## 5 | Results of Analysis

### 5.1 | Effect of Amount of Inherent Damping on Seismic Performance of Seismically Isolated Buildings

For the seismic performance evaluation in this study, the mean annual frequency of exceeding specific values of the peak floor acceleration, peak story drift ratio, peak residual story drift ratio,

and peak isolator horizontal displacement are considered. The selected EPDs are indicators of damage to structural and non-structural components, including the building contents. The peak isolator horizontal displacement is used to assess the potential failure of the seismic isolation system and the collapse of the building due to the failure of the isolation system. The mean annual frequency of an EDP exceeding a value  $y$ ,  $\lambda(\text{EDP} > y)$ , is computed based on NIST [29] and Lin et al. [30] as follows:

$$\lambda(\text{EDP} > y) = \sum_{i=1}^n P(\text{EDP} > y | Sa(T) = x_i) \cdot \lambda(Sa(T) = x_i) \quad (1)$$

$$\lambda(Sa(T) = x_i) = 0.5 \{ \lambda(Sa(T) > x_{i-1}) - \lambda(Sa(T) > x_{i+1}) \} \quad (2)$$

where  $n$  is the number of considered return periods (each related to seismic intensities) in terms of amplitudes of spectral accelerations,  $Sa(T)$  ( $n = 10$ ).  $x_i$  is the spectral acceleration at a period  $T$  for  $i^{\text{th}}$  return period. Also,  $\lambda(Sa(T) = x_i)$  is the rate of observing  $Sa(T)$  in some small range represented by the discrete amplitude  $x_i$ .  $P(\text{EDP} > y | Sa(T) = x_i)$  is the probability of the EDP that exceeds a value of  $y$  conditioned at the intensity of  $Sa(T) = x_i$ . The calculation of  $P(\text{EDP} > y | Sa(T) = x_i)$  depends on the

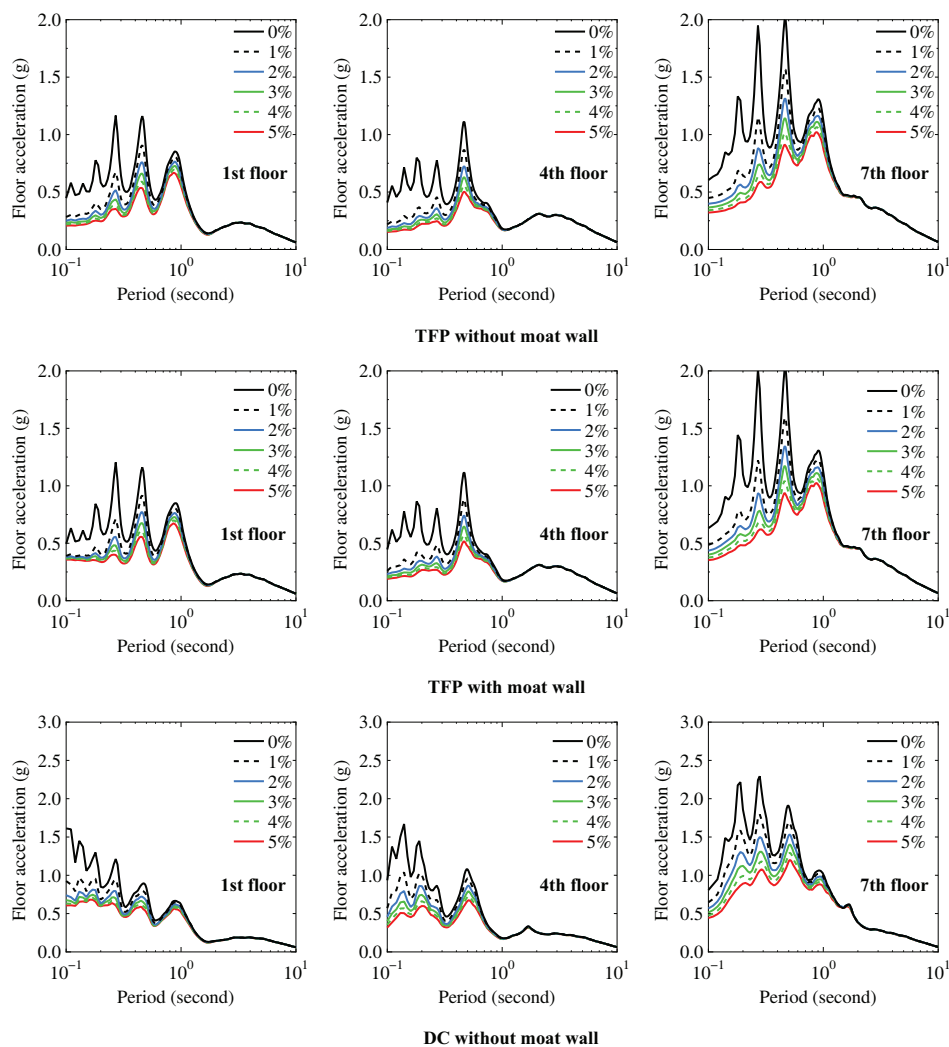


**FIGURE 9** | Mean floor acceleration spectra of seismically isolated buildings with special moment resisting frames (SMF) in 475-year return period ground motions for varying values of inherent damping modeled using “capped viscous damping”.

EDP. Readers should refer to the previous works of the authors for the detailed procedures for calculating the  $\lambda(EDP > y)$  [16, 18]. Figures 4 and 5 present the computed  $\lambda(EDP > y)$  for the seismically isolated buildings with SMF and SCBF, respectively. The results for both cases of damping model are shown but with different axes for the EDP (for the “modal damping” case, it increases to the right and for the “capped viscous damping” case, it increases to the left of each graph). The results for the two cases of damping model are virtually identical, leading to the conclusion that is the amount of damping, rather than the model of damping, that affects some results of seismic performance evaluation of seismically isolated buildings.

It is observed that there are significant variations in the computed  $\lambda(EDP > y)$  for the wide range of peak floor accelerations for both SMF and SCBF depending on the values of inherent damping. The variation of peak floor acceleration impacts the demand for non-structural components, such as suspended ceilings and sprinklers [32]. The amount of inherent damping has influence on the residual story drift in the SMF, but only for the DC system. This effect is significant only for small values of residual story drifts, which are below the threshold value of 0.005 (or 0.5%) and are unlikely to cause functionality issues [33, 34]. The likely reason for this effect

being observed only for the DC system is the behavior of the system, which exhibits abrupt changes in force while transitioning from loading to unloading. This behavior is known to promote the development of residual deformations [35]. TFP systems also exhibit abrupt changes in force but to a much lesser extent. A similar behavior could likely be accomplished in the DC system by using low friction on one of the two sliding surfaces [36], but that complicates the production of the isolators and has not been done in practice. The study of such systems is beyond the scope of this paper, which compares systems with identical frictional properties. The amount of inherent damping also affected the mean annual frequency of exceeding some values of peak story drift for SCBF, but this impact is limited to the small peak story drift, which is unlikely to cause functionality issues [34, 37, 38].

## 5.2 | Effect of Amount of Inherent Damping on Seismic Collapse Probabilities of Seismically Isolated Buildings

Collapse fragility curves, represented by cumulative distribution functions, were developed by fitting empirical collapse data to lognormal distributions. The empirical data consisted of the

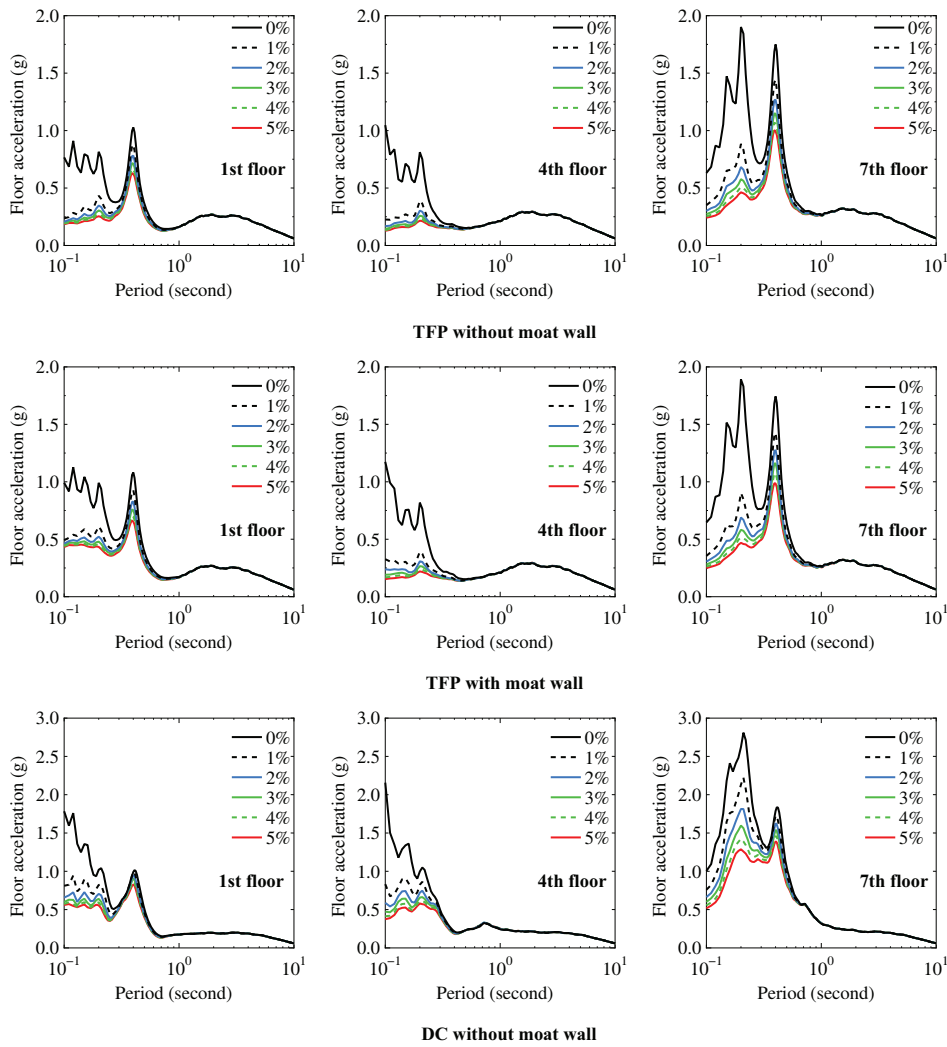


**FIGURE 10** | Mean floor acceleration spectra of seismically isolated buildings with special concentrically braced frames (SCBF) in 475-year return period ground motions for varying values of inherent damping modeled using “capped viscous damping”.

probability of collapse, calculated as the ratio of the number of collapse cases to the total number of analyses, across ten distinct values of seismic intensity, measured by the spectral acceleration at  $T$  (corresponding to return periods from 43 to 10,000 years). Failure of the analyzed structures was assumed when any of the following conditions occurred: (a) the maximum story drift ratio exceeded 0.05 [39] for buildings with SCBF and 0.1 [40] for buildings with SMF, (b) the isolator displacement exceeded  $D_{Ultimate}$  as shown in Figure 2, or (c) there was instability detected by the termination of the analysis program.

Figure 6 shows the collapse fragility curves of the isolated buildings for six different levels of inherent damping. Each of the fragility curves is characterized by the median,  $\widehat{S}a_{Collapse}(T_M)$ , which is the value of spectral acceleration at which the probability of collapse is 0.5, and the dispersion,  $\beta_{RTR}$ , which reflects the uncertainty of collapse capacity due to the record-to-record variability of the ground motions used in the nonlinear response history analysis. The results presented in Figure 6 shows that the inherent damping model and the level of inherent damping have very little, if any, impact on the collapse fragility curves for the isolated buildings.

While the fragility curves in Figure 6 show very small differences when using different values of inherent damping, it is important to compute the probabilities of collapse given the occurrence of the  $MCE_R$  [14]. The probability of collapse at  $MCE_R$  is used to assess the “acceptable” collapse performance of buildings in accordance with Tables 1.3–2 in the ASCE/SEI 7-16 standard [14]. These probabilities may vary depending on the amount of inherent damping used. The calculation of probabilities of collapse given the occurrence of the  $MCE_R$ ,  $P_{Collapse,MCE}$ , was computed as follows [40]:

$$P_{Collapse,MCE} = \int_0^1 \frac{1}{s\beta_{TOT}\sqrt{2\pi}} \exp\left[-\frac{(\ln s - ACMR)^2}{2\beta_{TOT}^2}\right] ds \quad (3)$$

$$ACMR = \frac{\widehat{S}a_{Collapse}(T)}{Sa_{MCE}(T)} \quad (4)$$

$$\beta_{TOT} = \sqrt{\beta_{RTR}^2 + \beta_{DR}^2 + \beta_{TD}^2 + \beta_{MDL}^2} \quad (5)$$

where  $\widehat{S}a_{Collapse}(T)$  is obtained from Figure 6,  $Sa_{MCE}(T)$  represents the spectral acceleration of  $MCE_R$  at  $T$  ( $Sa_{MCE}(T_M) = 0.246$  g for seismically isolated buildings),  $\beta_{TOT}$  denotes the total uncertainty,

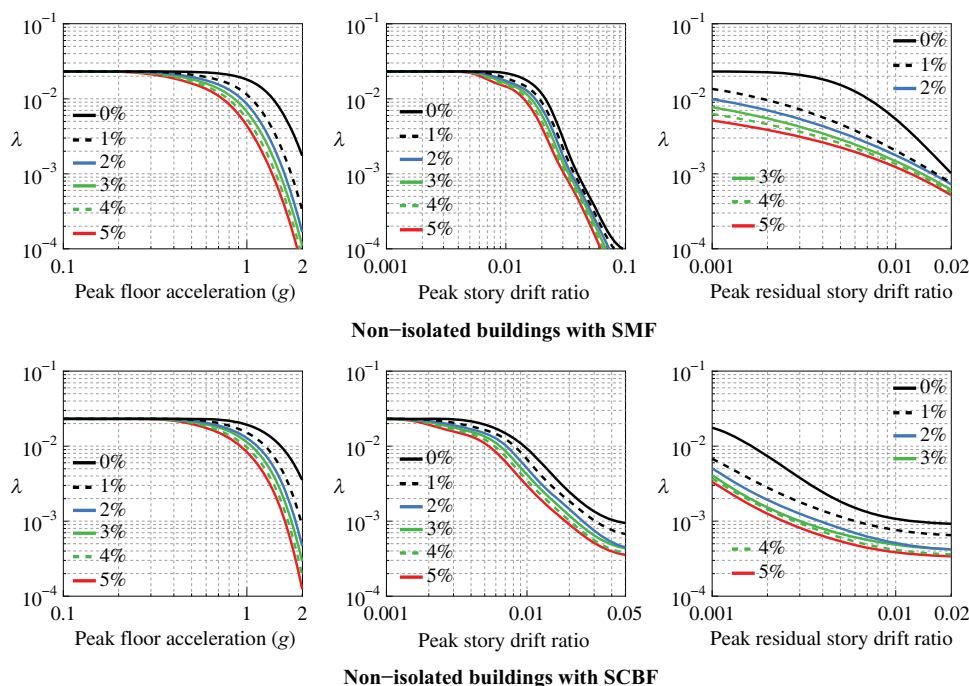


**FIGURE 11** | Mean annual frequencies of exceedance for various engineering demand parameters (EDP) of non-isolated buildings with special moment resisting frames (SMF) (top) and special concentrically braced frames (SCBF) (bottom) modeled using “modal damping”.

which is comprised of  $\beta_{DR}$  (design requirements-related collapse uncertainty),  $\beta_{TD}$  (test data-related collapse uncertainty), and  $\beta_{MDL}$  (modeling-related collapse uncertainty). The quality ratings and associated uncertainties applied are as follows: “Good” quality rating for modeling with  $\beta_{MDL} = 0.2$ , “Good” quality rating for test data with  $\beta_{TD} = 0.2$  and “Superior” quality rating for design requirements with  $\beta_{DR} = 0.1$ . These values are consistent with those used in [40, 41].

Table 1 presents the computed values of  $P_{Collapse, MCE}$  for each of the inherent damping values considered. Two values are provided, the first for the case of the “modal damping” model, and the second for the “capped viscous damping” model. Overall, the inherent damping model and the amount of inherent damping have a small effect on the probability of collapse at the  $MCE_R$ . It may be noted that three of the six studied systems have unacceptable probabilities of collapse, and one more (TFP without moat wall) barely exceeds the acceptable collapse probability of 0.1 in Tables 1.3–2 in the ASCE/SEI 7-16 and 7-22 standards. This is because the isolation system and superstructure design only meet the minimum design criteria of ASCE/SEI 7-16 or 7-22 and that acceptable performance would require larger isolator displacement capacities and smaller  $R$  factors [16, 17].

### 5.3 | Effect of Inherent Damping Model on Seismic Floor Acceleration Spectra of Seismically Isolated Buildings

It has been demonstrated that peak floor acceleration is the only EDP whose mean annual frequency of exceedance is significantly affected by the amount of inherent damping. This is important

because floor accelerations are indicators of potential damage to non-structural components, some of which are sensitive to accelerations [42–46]. Floor acceleration response spectra of seismically isolated buildings are presented for different values of inherent damping when using the “modal damping” and “capped viscous damping” models and for the set of 40 ground motions with a return period of 475 years. The presented spectra are the mean of the 40 analyses at three floors (1st, 4th, and the roof). According to [47], the 475-year return period intensity represents the earthquake scenario to assess resilience as defined by the San Francisco Planning and Urban Research Association. This scenario corresponds to a magnitude 7.2 earthquake, a reasonable expectation within a structure’s lifetime. Figures 7 and 8 present the mean floor acceleration spectra for seismically isolated buildings with SMF and SCBF, respectively, when using the “modal damping” model. Figures 9 and 10 present the results when using the “capped viscous damping” model. Results obtained for the case of the “capped viscous damping” model in Figures 9 and 10 are virtually the same as those of the “modal damping” model in Figures 7 and 8.

The data shows that floor acceleration spectra are significantly higher when inherent damping is zero. Even a small amount of damping (i.e., 1%) has an important effect in reducing the floor spectral accelerations, particularly for periods less than 1 s, where most non-structural components have their predominant period (C13.3.3 in ASCE/SEI 7-16 standard [14]). The results highlight the importance of accurately specifying inherent damping values in evaluating the seismic performance of acceleration-sensitive non-structural components. The insensitivity of inherent damping values in predicting floor spectral accelerations for periods longer than 1 s is attributed to the effectiveness of seismic isolation in reducing deformations in the superstructure.

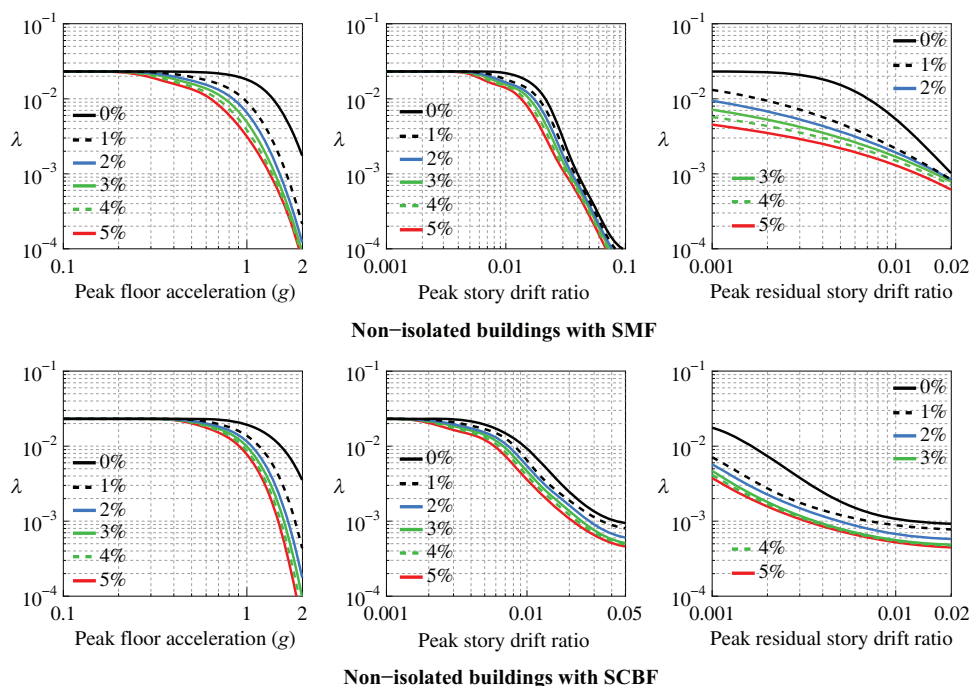


**FIGURE 12** | Mean annual frequencies of exceedance for various engineering demand parameters (EDP) of non-isolated buildings with special moment resisting frames (SMF) (top) and special concentrically braced frames (SCBF) (bottom) modeled using “capped viscous damping”.

Finally, although this study used a new column hinge model that can better simulate the cyclic deterioration behavior of columns [22] than the simpler bilinear-hysteresis model used in a previous study by the authors [13], this did not cause discrepancies in the results of analysis between the ones presented in this paper and the ones presented in [13]. The results presented in this section clearly showed how different amounts of inherent damping could affect the results of seismic performance evaluation of seismically isolated buildings that were unexplored in a previous study [13].

#### 5.4 | Effect of Amount of Inherent Damping on Seismic Performance of Non-Isolated Buildings

Figures 11 and 12 present the mean annual frequency of exceeding values of the peak floor acceleration, peak story drift ratio, and peak residual story drift ratio for the non-isolated buildings with SMF (top) and SCBF (bottom) for the cases of the “modal damping” and the “capped damping” models, respectively. The results for the two types of damping models are virtually identical.

Figures 11 and 12 show that the mean annual frequency of exceedance significantly depends on the values of inherent damping for all EDP and for a wide range of values of EDP. It does not depend on the models of damping. This contrasts with the results in Figures 4 and 5 for seismically isolated buildings, where the mean annual frequency of exceedance was generally unaffected by the amount of inherent damping, except for the case of the peak floor acceleration. Evidently, specifications for inherent damping in non-isolated buildings are more important in the seismic performance assessment of non-isolated buildings than of seismically isolated buildings.

#### 5.5 | Effect of Amount of Inherent Damping on Seismic Collapse Probabilities of Non-Isolated Buildings

Figure 13 presents collapse fragility curves for the non-isolated buildings constructed for the cases of “modal damping” (top) and “capped damping” (bottom) models of inherent damping. Criteria for collapse are the same as those for isolated buildings having excluded the criteria related to the isolators. The figure shows that the model of damping and the amount of inherent damping significantly affect the collapse fragility curves of non-isolated buildings. This contrasts with the collapse fragility curves for seismically isolated buildings in Figure 6, where neither the model nor the amount of inherent damping had any effect. This observation was expected, as seismically isolated buildings are not designed to prevent collapse through large inelastic deformation of the superstructure, whereas non-isolated buildings are designed to do so. Consequently, the inherent damping specified in the superstructure affects the behavior of the superstructure and thus influences collapse.

Use of the “modal damping” approach without capping [28] to model the inherent damping of non-isolated structures can result in “damping leakage” or “spurious damping” problems like those in isolated structures [13, 24] when the lateral force-resisting building elements, such as beams, columns, and braces, undergo large inelastic deformations. Accordingly, the “capped viscous damping” model, which reduces spurious damping, significantly reduced variability in collapse fragility curves. This type of damping is recommended for non-isolated buildings.

Table 2 presents values of the probability of collapse at the earthquake ground motion intensity of  $MCE_R$  as described previously in this paper to assess the “acceptable” collapse performance of

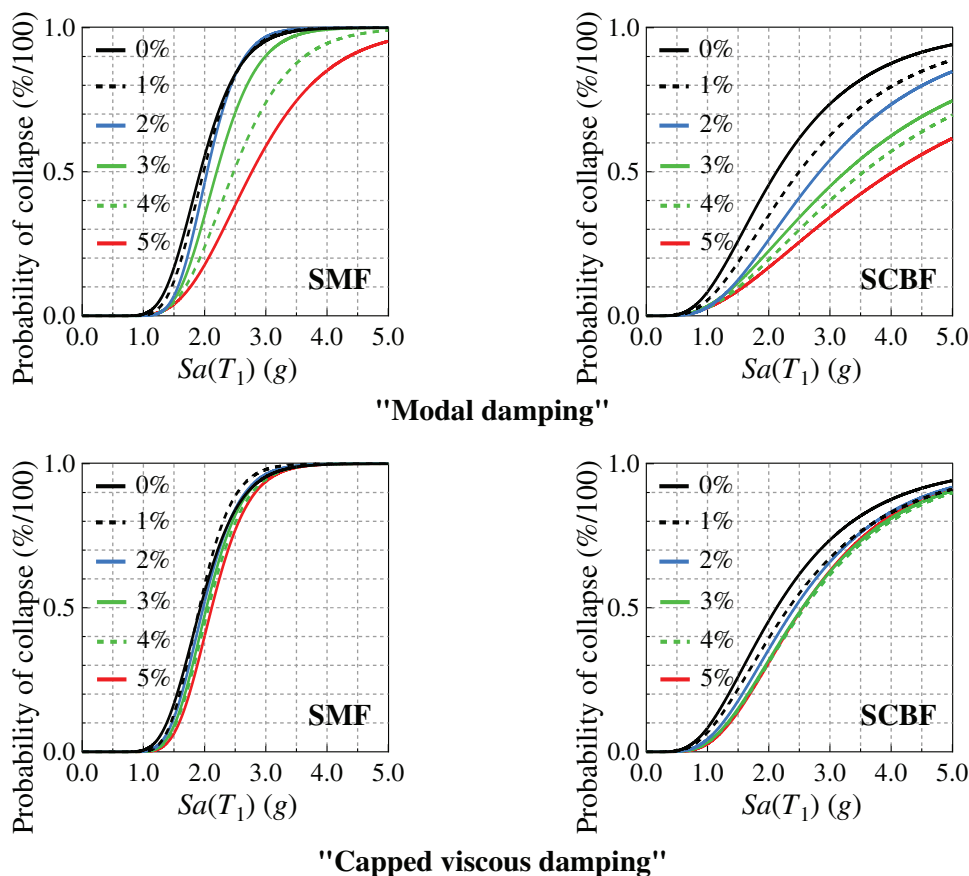


**FIGURE 13** | Collapse fragility curves of seismically isolated buildings for different amounts of inherent damping modeled using “modal damping” (top) and “capped viscous damping” (bottom).

**TABLE 2** | Collapse probabilities of non-isolated buildings in  $MCE_R$  ( $P_{Collapse, MCE_R}$ ).

Damping ratio	SMF (Modal damping/capped damping)	SCBF (Modal damping/capped damping)
0%	0.9/0.9	29.4/29.4
1%	0.6/0.6	22.3/24.4
2%	0.3/0.3	16.5/22.1
3%	0.3/0.4	14.5/19.6
4%	0.3/0.4	12.5/19.0
5%	0.2/0.3	11.0/18.8

Abbreviations: SCBF, special concentrically braced frames; SMF, special moment resisting frames.

buildings using Equations (3)–(5). In Equation (4),  $Sa_{MCE}(T) = 0.756$  g and 1.500 g were considered for non-isolated buildings with SMF and SCBF, respectively [19]. Also, for the non-isolated structure with SCBF,  $\beta_{MDL} = 0.2$ ,  $\beta_{TD} = 0.2$ , and  $\beta_{DR} = 0.2$  were used based on Chen and Mahin [48] and NIST [49]. For the non-isolated structure with SMF,  $\beta_{MDL} = 0.2$ ,  $\beta_{TD} = 0.2$ , and  $\beta_{DR} = 0.1$  were selected based on NIST [49] and Elkady and Lignos [50]. Two values are shown in Table 2, the first for the case of the “modal damping” model and the second for the case of “capped

viscous damping” model. As seen in the table, the probabilities of collapse at the  $MCE_R$  for the non-isolated SMF are too small, so while there is the effect of the model of inherent damping and its amount, it is not important. However, the effects of the damping model and its amount on the collapse probabilities of the non-isolated SCBF are important. It is inferable that assigning different values of inherent damping could lead to either acceptable or unacceptable collapse probabilities for non-isolated buildings. Although differences in collapse probabilities at  $MCE_R$  for different inherent damping values remain notable, they are smaller when the “capped viscous damping” model is used.

### 5.6 | Effect of Inherent Damping Model on Seismic Floor Acceleration Spectra of Non-Isolated Buildings

Like Section 5.3 of this paper, floor acceleration spectra were generated to examine the impact of different amounts of inherent damping on the performance of acceleration-sensitive non-structural components in non-isolated buildings. Figures 14 and 15 present the mean floor acceleration spectra for non-isolated buildings with SMF and SCBF for the 1st, 4th, and 7th floors for the case of the “modal damping” and “capped viscous damping” models, respectively. The results from the case “capped viscous damping” model show that the variation of the floor spectral accelerations at large periods is slightly smaller than the results from the case “modal damping” model.

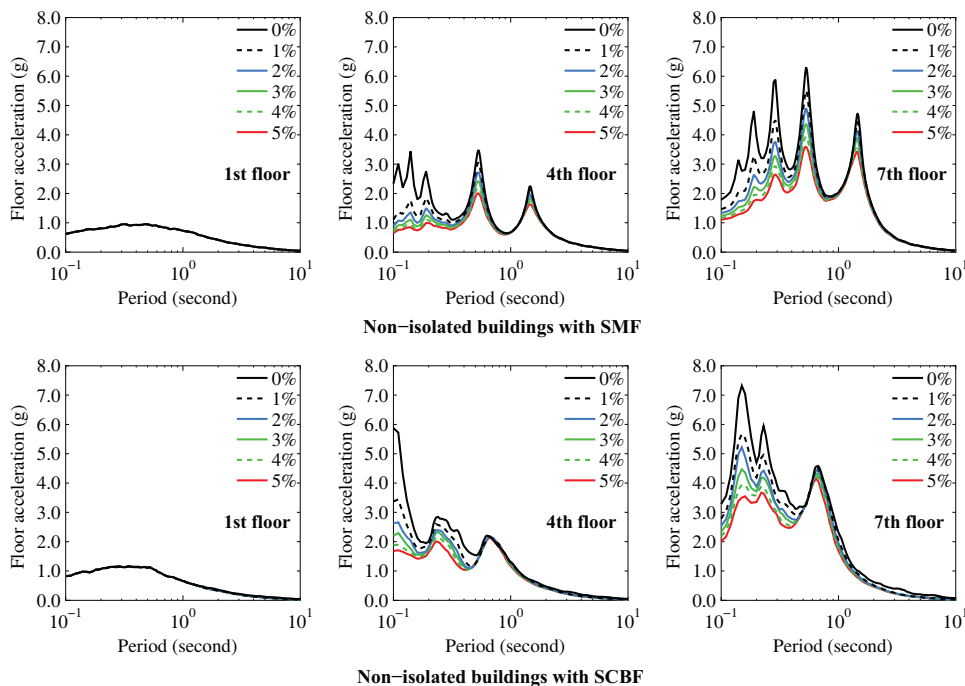


**FIGURE 14** | Mean floor acceleration spectra of seismically isolated buildings with special moment resisting frames (SMF) (top) and special concentrically braced frames (SCBF) (bottom) modeled using “modal damping” in 475-year return period ground motions.

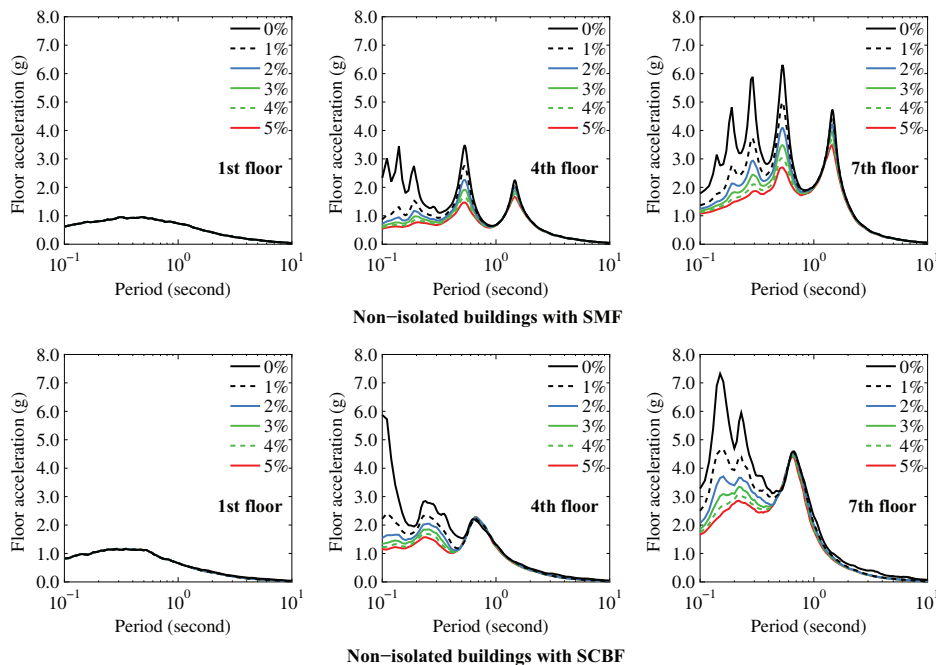


**FIGURE 15** | Mean floor acceleration spectra of seismically isolated buildings with special moment resisting frames (SMF) (top) and special concentrically braced frames (SCBF) (bottom) modeled using “capped viscous damping” in 475-year return period ground motions.

This difference is attributed to the reduced amount of spurious damping under large structural deformations when using the “capped viscous damping” model as compared to the “modal damping”, as previously discussed in this article.

The data indicate that floor acceleration spectra are significantly higher when inherent damping is zero compared to when inherent damping is present ( $>0$ ). Unlike the floor acceleration spectra

observed in seismically isolated buildings, varying inherent damping affects not only the spectra for periods below 1 s but also periods beyond 1 s, especially at higher floors such as the 7th floor. This highlights the importance of accurately specifying inherent damping values when evaluating the seismic performance of acceleration-sensitive non-structural components, regardless of their predominant period. It is noted that varying inherent damping does not impact the floor acceleration spectra on the

first floor, as the building model assumes the first floor is rigidly attached to the ground and moves with it.

## 6 | Conclusions

The conclusions of this study apply for a sample of seismically isolated and comparable non-isolated buildings designed based on the minimum criteria of ASCE/SEI 7-16 [14] (also ASCE/SEI 7-22 [15]) and which have been analyzed to determine statistical response quantities that are useful in assessing seismic performance, including seismic collapse performance. The amount of inherent damping assumed for the structures (superstructure for the isolated buildings) varied between zero and 5% in each mode of vibration, modeled using either the “modal damping” or the “capped viscous damping” method. The seismic isolation systems considered are sliding friction pendulum type. The conclusions are:

1. For seismically isolated buildings, only the peak floor acceleration was significantly affected by the amount of inherent damping, whereas the inherent damping model did not have any important effects. Examination of floor acceleration spectra showed that the impact of the amount of damping was important for non-structural components with periods below 1 s. Therefore, when the analysis of seismically isolated buildings includes analysis of acceleration-sensitive non-structural components with periods below 1 s, the amount of inherent damping should be carefully selected.
2. The collapse probability of seismically isolated buildings during extreme earthquake events is not affected by the amount of inherent damping or the model of inherent damping. This finding simplifies the modeling process for inherent damping in seismically isolated buildings when the focus of nonlinear response history analysis is solely on evaluating collapse performance.
3. For seismically isolated buildings, “modal damping” and “capped damping” are reliable inherent damping models if they are applied, as shown in this work, for avoiding “spurious damping” problems.
4. For non-isolated buildings, the floor accelerations (including peak values and floor spectral values), the peak story drift ratios, the residual story drift ratios, and the probabilities of collapse in the maximum earthquake are significantly affected by the amount of inherent damping and the model of damping. It is recommended that the “capped viscous damping” model is used as it mitigated “spurious damping” problems and had smaller effects on the computed statistics of response parameters when the amount of damping was varied.

The results are valid for the isolation systems studied and do not necessarily apply to all isolation systems.

---

### Data Availability Statement

The data that support the findings of this study are available from the corresponding author upon reasonable request.

## References

1. N. Satake, K. Suda, T. Arakawa, A. Sasaki, and Y. Tamura, “Damping Evaluation Using Full-Scale Data of Buildings in Japan,” *Journal of Structural Engineering* 129, no. 4 (2003): 425–563.
2. Applied Technology Council (ATC). *ATC-72-1: Modeling and Acceptance Criteria for Seismic Design and Analysis of Tall Buildings* (Applied Technology Council, 2010), 242.
3. D. Bernal, M. Döhler, S. M. Kojidi, K. Kwan, and Y. Liu, “First Mode Damping Ratios for Buildings,” *Earthquake Spectra* 31, no. 1 (2015): 367–381.
4. A. S. Veletsos and J. W. Meek, “Dynamic Behaviour of Building-Foundation Systems,” *Earthquake Engineering & Structural Dynamics* 3, no. 2 (1974): 121–138.
5. C. Cruz and E. Miranda, “Insights Into Damping Ratios in Buildings,” *Earthquake Engineering & Structural Dynamics* 50, no. 3 (2021): 916–934.
6. R. K. Goel and A. Chopra, *Vibration Properties of Buildings Determined From Recorded Earthquake Motions. UCB/EERC Report 97/14* (University of California, Berkeley, 1997), 286.
7. W. P. Fritz, N. P. Jones, and T. Igusa, “Predictive Models for the Median and Variability of Building Period and Damping,” *Journal of Structural Engineering* 135, no. 5 (2009): 576–586.
8. C. Cruz and E. Miranda, “Damping Ratios of the First Mode for the Seismic Analysis of Buildings,” *Journal of Structural Engineering* 147, no. 1 (2021): 04020300.
9. C. Cruz and E. Miranda, “Reliability of Damping Ratios Inferred From the Seismic Response of Buildings,” *Engineering Structures* 184 (2019): 355–368.
10. J. P. Stewart, J. P. Conte, and I. D. Aiken, “Observed Behavior of Seismically Isolated Buildings,” *Journal of Structural Engineering* 125, no. 9 (1999): 943–1082.
11. M. C. Constantinou and M. C. Kneifati, “Dynamics of Soil-Base-Isolated-Structure Systems,” *Journal of Structural Engineering* 114, no. 1 (1988): 211–221.
12. Pacific Earthquake Engineering Research Center (PEER). *Guidelines for Performance-Based Seismic Design of Tall Buildings. TBI 2017* (Pacific Earthquake Engineering Research Center, 2017), 147.
13. S. Kitayama and M. C. Constantinou, “Effect of Modeling of Inherent Damping on the Response and Collapse Performance of Seismically Isolated Buildings,” *Earthquake Engineering & Structural Dynamics* 52, no. 3 (2023): 571–592.
14. American Society of Civil Engineers (ASCE). *ASCE/SEI 7-16 Minimum Design Loads and Associated Criteria for Buildings and Other Structures* (American Society of Civil Engineers, 2017), 822.
15. American Society of Civil Engineers (ASCE). *ASCE/SEI 7-22 Minimum Design Loads and Associated Criteria for Buildings and Other Structures* (American Society of Civil Engineers, 2021), 1046.
16. S. Kitayama and M. C. Constantinou, *Seismic Performance Assessment of Seismically Isolated Buildings Designed by the Procedures of ASCE/SEI 7. Report MCEER-18-0004* (Multidisciplinary Center for Earthquake Engineering Research, University at Buffalo, The State University of New York, 2018), 164.
17. S. Kitayama and M. C. Constantinou, “Collapse Performance of Seismically Isolated Buildings Designed by the Procedures of ASCE/SEI 7,” *Engineering Structures* 164 (2018): 243–258.
18. S. Kitayama and M. C. Constantinou, “Probabilistic Seismic Performance Assessment of Seismically Isolated Buildings Designed by the Procedures of ASCE/SEI 7 and Other Enhanced Criteria,” *Engineering Structures* 179 (2019): 566–582.
19. Structural Engineers Association of California (SEAOC). *2012 IBC SEAOC Structural/Seismic Design Manual Volume 5: Examples for*

- Seismically Isolated Buildings and Buildings With Supplemental Damping* (Structural Engineers Association of California, 2014), 170.
20. W. J. McVitty and M. C. Constantinou, *Property Modification Factors for Seismic Isolators: Design Guidance for Buildings*. Report MCEER-15-0005 (Multidisciplinary Center for Earthquake Engineering Research, University at Buffalo, The State University of New York, 2015), 242.
  21. F. T. McKenna, *Object-Oriented Finite Element Programming: Frameworks for Analysis, Algorithms and Parallel Computing*. PhD Dissertation (University of California, Berkeley, 1997), 265.
  22. D. G. Lignos, A. R. Hartloper, A. Elkady, G. G. Deierlein, and R. Hamburger, "Proposed Updates to the ASCE 41 Nonlinear Modeling Parameters for Wide-Flange Steel Columns in Support of Performance-based Seismic Engineering," *Journal of Structural Engineering* 145, no. 9 (2019): 04019083.
  23. L. F. Ibarra and H. Krawinkler, *Global Collapse of Frame Structures Under Seismic Excitations*. John A. Blume Earthquake Engineering Center Technical Report 152 (Stanford University, 2005), 349.
  24. A. A. Sarlis and M. C. Constantinou, *Modeling Triple Friction Pendulum Isolators in Program SAP2000*. Report Distributed to the Engineering Community Together With Example Files (University at Buffalo, State University of New York, 2010), 55.
  25. X. Qian, A. K. Chopra, and F. McKenna, *Modeling Viscous Damping in Nonlinear Response History Analysis of Steel Moment-frame Buildings: Design plus Ground Motions*. Revision 1.0. PEER 2020/01 (University of California, Berkeley, 2020), 143.
  26. J. F. Hall, "Problems Encountered From the Use (or Misuse) of Rayleigh Damping," *Earthquake Engineering & Structural Dynamics* 35, no. 5 (2006): 525–545.
  27. J. F. Hall, "Performance of Viscous Damping in Inelastic Seismic Analysis of Moment-frame Buildings," *Earthquake Engineering & Structural Dynamics* 47, no. 14 (2018): 2756–2776.
  28. A. K. Chopra and F. McKenna, "Modeling Viscous Damping in Non-linear Response History Analysis of Buildings for Earthquake Excitation," *Earthquake Engineering & Structural Dynamics* 45, no. 2 (2016): 193–211.
  29. National Institute of Standards and Technology (NIST). *Selecting and Scaling Earthquake Ground Motions for Performing Response-history Analysis*. NIST GCR 11-917-15 (National Institute of Standards and Technology, 2011), 256.
  30. T. Lin, C. B. Haselton, and J. W. Baker, "Conditional Spectrum-Based Ground Motion Selection. Part I: Hazard Consistency for Risk-based Assessments," *Earthquake Engineering & Structural Dynamics* 42, no. 12 (2013): 1847–1865.
  31. F. Jalayer, *Direct Probabilistic Seismic Analysis: Implementing Non-Linear Dynamic Assessments*. PhD Dissertation (Stanford University, 2003), 272.
  32. National Institute of Standards and Technology (NIST). *Recommendations for Improved Seismic Performance of Nonstructural Components*. NIST GCR 18-917-43 (National Institute of Standards and Technology, 2018), 309.
  33. J. McCormick, H. Aburano, M. Ikenaga, and M. Nakashima, "Permissible Residual Deformation Levels for Building Structures Considering both Safety and human Elements," paper presented at the 14th World Conference on Earthquake Engineering, 2008, Beijing, China.
  34. Federal Emergency Management Agency (FEMA). *Seismic Performance Assessment of Buildings*. Report FEMA P-58. Volume 1 – Methodology, 2nd ed. (Federal Emergency Management Agency, 2018), 340.
  35. C. P. Katsaras, T. B. Panagiotakos, and B. Koliass, "Restoring Capability of Bilinear Hysteretic Seismic Isolation Systems," *Earthquake Engineering & Structural Dynamics* 37, no. 4 (2008): 495–658.
  36. D. Fenz and M. C. Constantinou, "Behavior of the Double Concave Friction Pendulum Bearing," *Earthquake Engineering & Structural Dynamics* 35, no. 11 (2006): 1321–1451.
  37. Kitayama and H. Cilsalar, "Seismic Loss Assessment of Seismically Isolated Buildings Designed by the Procedures of ASCE/SEI 7-16," *Bulletin of Earthquake Engineering* 20 (2022): 1143–1168.
  38. S. Kitayama, E. A. M. Moncayo, and A. Athanasiou, "Inspection and Repair Considerations for Downtime Assessment of Seismically Isolated Buildings," *Soil Dynamics and Earthquake Engineering* 164 (2023): 107618.
  39. R. Sabelli, C. W. Roeder, and J. F. Hajjar, *Seismic Design of Steel Special Concentrically Braced Frame Systems—A Guide for Practicing Engineers*. NEHRP Seismic Design Technical Brief No. 8, NIST GCR 13-917-24 (National Institute of Standards and Technology, 2013), 36.
  40. Federal Emergency Management Agency (FEMA). *Quantification of Building Seismic Performance Factors*. Report FEMA P695 (Federal Emergency Management Agency, 2009), 422.
  41. A. Masroor, "Assessing the Collapse Probability of Base-isolated Buildings Considering Pounding to Moat Walls Using the FEMA P695 Methodology," *Earthquake Spectra* 31, no. 4 (2015): 2069–2086.
  42. E. Pavlou and M. C. Constantinou, "Response of Nonstructural Components in Structures With Damping Systems," *Journal of Structural Engineering* 132, no. 7 (2006): 1108–1117.
  43. E. D. Wolff, C. Ipek, M. C. Constantinou, and M. Tapan, "Effect of Viscous Damping Devices on the Response of Seismically Isolated Structures," *Earthquake Engineering & Structural Dynamics* 44, no. 2 (2015): 185–198.
  44. E. Miranda and S. Taghavi, "A Comprehensive Study of Floor Acceleration Demands in Multi-story Buildings," paper presented at the ATC and SEI Conference on Improving the Seismic Performance of Existing Buildings and Other Structures, December 9–11, 2009, San Francisco, CA, USA.
  45. V. Vukobratović and P. Fajfar, "A Method for the Direct Estimation of Floor Acceleration Spectra for Elastic and Inelastic MDOF Structures," *Earthquake Engineering and Structural Dynamics* 45, no. 15 (2016): 2495–2511.
  46. H. Anajafi and R. A. Medina, "Evaluation of ASCE 7 Equations for Designing Acceleration-Sensitive Nonstructural Components Using Data From Instrumented Buildings," *Earthquake Engineering & Structural Dynamics* 47, no. 4 (2018): 1075–1094.
  47. C. Molina Hutt, I. Almufti, M. Willford, and D. Deierlein, "Seismic Loss and Downtime Assessment of Existing Tall Steel-Framed Buildings and Strategies for Increased Resilience," *Journal of Structural Engineering* 142, no. 8 (2016): C4015005.
  48. C. H. Chen and S. A. Mahin, *Performance-Based Seismic Demands Assessment of Concentrically Braced Steel Frame Buildings*. PEER 2012/103 (University of California, Berkeley, 2012), 191.
  49. National Institute of Standards and Technology (NIST). *NEHRP Seismic Design Technical Brief No.4: Nonlinear Structural Analysis for Seismic Design: A Guide for Practicing Engineers*. NIST GCR 10-917-5 (National Institute of Standards and Technology, 2010), 32.
  50. A. Elkady and D. G. Lignos, "Effect of Gravity Framing on the Overstrength and Collapse Capacity of Steel Frame Buildings With Perimeter Special Moment Frames," *Earthquake Engineering & Structural Dynamics* 44, no. 8 (2014): 1289–1307.